Investigation of solitary quasishock compression waves in a velocity-modulated ion beam

V. F. Virko and G. S. Kirichenko

Nuclear Research Institute of the Ukrainian Academy of Sciences
(Submitted 24 April 1979)
Zh. Eksp. Teor. Fiz. 77, 1943–1950 (November 1979)

The dynamics of formation of a solitary density blob produced in an electron-neutralized ion beam whose velocity is increased jumpwise is investigated. Two ion-sound perturbation packets are excited at the velocity discontinuity site. With increasing discontinuity amplitude, the packets are transformed into two shock waves of the ion-sound type which propagate along the beam in opposite directions. When the velocity-modulation amplitude exceeds the ion-sound velocity by ~2.5 times, the merging of the wave fronts in the beam results in formation of a solitary high-amplitude quasishock wave of width comparable with the electron Debye radius. The nonstationary stage of this process is accompanied by anomalous acceleration and deceleration of ion groups that do not stem from the turbulence.

PACS numbers: 41.80.Gg

Research aimed at obtaining pulsed ionic beams of high density has expanded greatly of late. For example, in connection with the problem of controlled thermonuclear fusion, the possibility of inertial containment and heating of a solid target by dense ion beams is now under discussion. The traditional method of increasing the density in the beam is to use phase focusing with modulation of the beam-particle velocities. The beam of positive ions whose space charge is neutralized by electrons constitutes a plasma system (if the Debye screening radius does not exceed the beam dimensions). In this case the dynamics of the phase focusing of the ions can greatly differ from the analogous process in systems of the electron klystron type. The process of formation of ion blobs following a jumplike increase of the ion-beam velocity is presently under experimental investigation. It has been shown that such a blob is a solitary quasishock compression wave with fronts of width comparable with the Debye radius of the electrons. The optimal conditions for increaseing the current density in the ion blob were determined.

EXPERIMENTAL SETUP

The experimental setup (Fig. 1) consisted of a cylindrical copper chamber, in the end face of which was placed a surface-ionization source of potassium ions. The source consisted of an incandescent tungsten emitter disk *1*, a unit that bombards the emitter surface with a beam of potassium atoms, and an accelerating grid *2* (grid—emitter distance 0.5 mm). The grid was electrically connected to the chamber, and the ion-accelerating voltage was applied to the emitter. The space charge of the ion beam was compensated by electrons from incandescent filaments of a neutralizer *3*. On the top of Fig. 1 is shown schematically the distribution, measured with an incandescent probe, of the static potential along the system axis. The chamber length was 36 cm, the diameter 10 cm, the tungsten-disk diameter 4 cm, the ion-beam energy $\varepsilon_0 = 20$—200 eV, the current beam could reach 3 mA [ion concentration $n_0 = (1\text{–}4) \cdot 10^8$ cm^{-3}], the pressure in the chamber under operating conditions was ~ 10^{-5} Torr, and the plasma-column potential containing the electrons was $\varphi_0 \approx 10$ V relative to the chamber walls. The electron temperature T_e in the investigated ion-beam plasma could be regulated in the range 0.3–1.2 eV by varying the neutralizer operating regime. The ion temperature on the surface of the incandescent emitter was $T_{i0} \lesssim 0.2$ eV, and the corresponding scatter of the velocities of the beam was equivalent to a longitudinal particle temperature $T_{i\parallel} \approx T_{i0}^2/4\varepsilon_0 \sim 10^{-4}$ eV and to a transverse temperature $T_{i\perp} \approx T_{i0}$.

The ion-beam velocity was modulated by applying to the emitter at the instant $t = 0$, on top of the dc accelerating voltage U_1, a switching pulse from generator *4* with adjustable amplitude $\Delta U = 0$–7 eV and a rise time 0.1 μsec. As a result, the ion-beam velocity increased jumpwise from V_1 to $V_2 = V_1 + \Delta V$. The current density increased in this case by not more than 20% and this, when account is taken of the increase of the velocity, correspond to practically no change in the beam-ion concentration. In the region of the velocity break, the accelerated part of the beam moved ahead of the slower one, thus leading to formation of a density perturbation that moved together with the beam ions along the flight path. At a distance x from the source, the ion-density perturbation was registered with a movable electrostatic analyzer *5* and an oscilloscope *6* having a resolution time 0.1 μsec.

The energy distribution of the ions in the beam at an arbitrary instant of time was determined from the collector-current oscillograms obtained at different potentials of the analyzing grid. The alternating potential in the beam was estimated with the aid of a glass-coated (insulated) probe *7*, an amplifier with high input resistance, and an oscilloscope.

We use henceforth the following notation: ε_1 and V_1

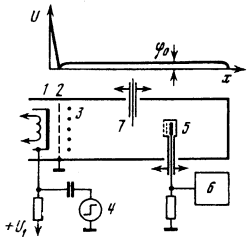

FIG. 1. Diagram of experimental setup.

 0038-5646/79/110923-04$02.40 © 1980 American Institute of Physics

are the energy and velocity of the slower beam 1 moving ahead of the velocity break; ε_2 and V_2 are the energy and velocity of the faster beam 2, which moves past the break; $\Delta V = V_2 - V_1$ is the difference between the velocities of the beams, $V_0 = (V_1 + V_2)/2$ is the average ion velocity, φ is the variable potential produced in the region of the velocity break, $n_{i,e}$ is the concentration of the ions or electrons; d_e, and v_{Te} are the Debye radius and the thermal velocity of the electrons, C_s is the ion-sound velocity, and e and m_i are the charge and mass of the ion.

EXPERIMENTAL RESULTS

Figure 2 shows the ion-current oscillograms obtained at a distance $x = 36$ cm from the source at different values of the beam-velocity modulation amplitude. The curves actually show the spatial structure of the ion-density perturbation carried by the beam after the lapse of the flight time $t_0 = x/V_0$. A characteristic feature at small beam amplitudes is the appearance of two systems of waves propagating along the beam in opposite directions from the coordinate of the initial perturbation (curves *1* and *2*). With increasing ΔU there are formed on the fronts of the packets density jumps (curves *3* and *4*) whose relative velocity (pulse width in Fig. 2) decreases until they merge (curve *5*). A narrow solitary ion blob is then produced in the beam. Further increase of ΔU leads again to a density distribution with "diverging" gently sloping fronts (curves *6*, *7*, *8*).

Figure 3 shows the temporal (i.e., spatial) beam-ion energy distributions corresponding to the indicated three characteristic ranges of the modulation amplitude. The $F(\varepsilon)$ curves were obtained with an electrostatic analyzer, followed by differentiation of the delay characteristics. The data on Fig. 3 are given for a number of instants of time close to t_0.

The front velocities determined by measuring the time of flight (see Fig. 2), are shown as functions of ΔV in Fig.4. The left-hand (faster) and right-hand fronts of Fig. 2 correspond respectively to light and dark circles in Fig. 4, where straight lines represent the beam velocities V_1 and V_2.

In the subsequent analysis of the experimental data it is convenient to use a system of coordinates $x' = x - V_0 t$ that moves with the average beam velocity.

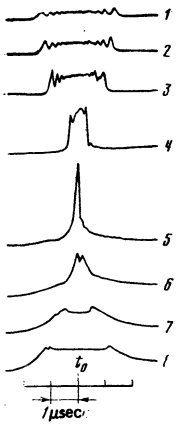

FIG. 2. Oscillograms of the ion current at various values of the modulation amplitude. Curves 1—8 correspond to ΔU values 2, 3, 5, 13, 30, 35, 40, and 50 V; $t_0 \approx 18$ μsec, $U_1 = 90$ V, $T_e = 1.2$ eV.

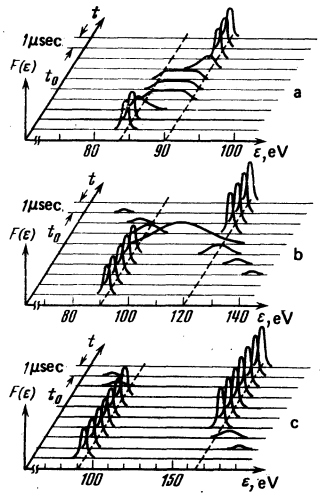

FIG. 3. Distribution function of beam-ion energy near the velocity-break point, corresponding to different modulation amplitudes. The dashed lines indicate the beam energies ε_1 and ε_2.

1. As seen from Fig. 2 (curves *1* and *2*), at small amplitude ΔU of the modulating signal the increase of the density produced in the region of the velocity break can be regarded as an instantaneous one-dimensional source of perturbation. Two waves propagate from it in opposite directions, with a phase that varies in space and time, a fact reflecting the dispersion properties of the medium. Under the conditions of the described experiment, the wave process is of the ion-sound type. From oscillograms similar to curve *1* of Fig. 2 it is possible to obtain the dependence of the propagation velocity of the wave packets in the corresponding system of coordinates x' on the wave number k, as shown in Fig. 5. Curve *1* of this figure shows the calculated phase velocity of one-dimensional ion sound

$$v_{ph} = \omega/k = C_s/(1+k^2d_e^2)^{1/2}$$

at the corresponding parameters of the system ($T_e = 1,2$ eV, $n_0 = 1,5 \cdot 10^8$ cm^{-3}), while curve 2 shows the group velocity

$$v_{gr} = \partial\omega/\partial k = v_{ph}(1+k^2d_e^2)^{-1}.$$

The experimental points agree well with the dispersion of ion-sound waves. The velocity of the linear ion sound determined in this manner (at small values of ΔU) is plotted in Fig. 4 (the dashed lines $V_2 - C_s$ and $V_1 + C_s$). With increasing modulation amplitude, the packets of the ion-sound perturbations, propagating along the beam, form two shock waves (density discontinuities) with fronts whose width is comparable with the Debye radius ($d_e \sim 0.1$ cm). The oscillations behind the

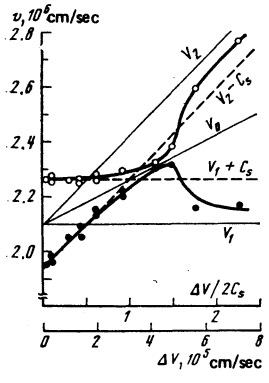

FIG. 4. Propagation velocities of the fronts of the density perturbation due to pulsed modulation of the ion-beam velocity.

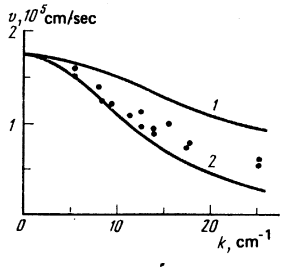

FIG. 5. Dispersion of the waves excited by a slow-amplitude velocity-modulation pulse.

front of each of the waves, as seen from Fig. 2, reflect the structure of the field of the ion-sound packets. The growth of the amplitude of the density discontinuity with increasing ΔV leads to an increase of the velocity of the fronts (see Fig. 4) relative to the corresponding ion background: the faster front (light circles) moves along the beam 1, and the slower (dark circles) along beam 2. Behind the front of each of the shock waves (within the limits of the density pulse on Fig. 2, curves *2, 3, 4*) the distribution of the ion velocities covers the entire range from V_1 to V_2. The latter is shown in Fig. 3a.

2. From Fig. 2 (curve *5*) and Fig. 4 it is seen that at $\Delta V \approx 2.6C_s$, at the point of the ion-beam velocity break ($x' = 0$), the joining the fronts of the two shock waves produces a solitary density peak with width ~3–5 Debye radii. The corresponding Mach number for the solitary wave is $M = 1.3$ relative to each of the beams. The Mach number was independent of the absolute value of the electron temperature in the entire range of its variation in the described experiments. The ratio of the ion concentration in the cluster and in the unperturbed beam was $n_i/n_0 \approx 5$–7. The electron-density ratio obtained with an electrostatic analyzer was $n_e/n_0 \approx 3$.

Figure 6 shows oscillograms of the ion current of the cluster, obtained at various distances from the ion source. The ion density increases in space over a path length ~10 cm, and then remains practically unchanged, i.e., a stationary state of the solitary density wave is reached. Oscillogram *6* (Fig. 6) shows the distribution of the potential in the investigated wave ($x = 20$ cm).

The limiting values of the potential φ_m in an ion-sound wave moving with velocity v are determined, as is well known, by the condition of ion reflection from the wave front, $m_i v^2/2 = e\varphi_m$. In the investigated solitary wave (see Fig. 4) $v = \Delta V/2 \approx 1,3C_s$, i.e., $e\varphi_m \approx 0,85T_e$. The amplitudes of the potential in the stationary blob agrees with this value within the limits of the measurement error ($\varphi_m \approx 1$–1.2 V, see Fig. 6, curve 6).

Figure 3b shows the distribution of the ion velocities near the point of the velocity break under conditions when a solitary wave is produced in the beam. The density peak ($t = t_0$) represents particles from the entire ΔV range (from V_1 to V_2) with a distribution maximum in the region of the average velocity V_0. The continuity of the distribution in a laminar wave can be attributed to the fact that in the described experiment the total length of the beam drift space did not exceed substantially the region of formation (amplitude growth) of the wave. In the nonstationary case ($d\varphi(x)/dt \neq 0$) it is natural to have a broadening of the ion velocity distribution on the phase plane.

In the investigated system, the ions can be reflected from either the leading front (ions of sort 1 are reflected) or the trailing edge (ions of beam 2 are reflected) of the stationary ($\varphi_m(t) = \text{const}$) potential "hump" moving with velocity $\Delta V/2$. As a result of the partial reflection, the velocity of a group of ions of beam 1, increases from V_1, in the laboratory frame to a value V_2, forming a "precursor" ahead of the solitary wave. A similar phenomenon takes place also on the trailing edge, where the reflection of the faster beam forms a flux that is symmetrical to the "precursor" and lags the solitary wave. These fluxes are seen in Fig. 2 (curve *5*). However, as shown by oscillograms *2* and *3* of Fig. 6, the ion fluxes leading and lagging the blob are produced already during the stage of formation of the solitary wave. An analysis of the velocity distribution (Fig. 3b) indicates that some of the ions that precede the wave have energies greatly exceeding the energy ε_2, of the faster beam, while the lagging ions have energies $\varepsilon < \varepsilon_1$. These ions are produced when $\varphi(t) < \varphi_m$, and are not reflected by the fronts, but $d\varphi/dt > 0$. A beam of ions with velocity $\Delta V/2$, on passing through a potential "hump" that increases with time, undergoes a velocity increase by an amount

$$\Delta v \approx \frac{e}{m_i}\frac{d\varphi}{dt}\frac{\Delta t}{\Delta V/2},$$

where Δt is the time of motion in the region of the potential localization: $\Delta t \approx 2\delta/\Delta V$ (δ is the width of the solitary wave). An estimate of $d\varphi/dt$ can be obtained from the value of the limiting potential in the wave φ_m and its growth time τ (see Fig. 6), i.e.,

$$\Delta v \approx \frac{e\delta\varphi_m}{m_i(\Delta V/2)^2\tau},$$

and under the experimental conditions ($\delta \approx 2$ cm, $\varphi_m \approx 1$B, $\Delta V/2 = 2,2 \cdot 10^5$ cm/sec, $\tau \approx 6 \cdot 10^{-6}$ sec) $\Delta v \approx 1,4 \cdot 10^5$ cm/sec, which corresponds to the beam acquiring in the laboratory frame an energy $\Delta\varepsilon \approx 2\varepsilon_0 \Delta V/V_0 = 13$ eV ($\varepsilon_0 = 100$ eV). The experimental values ~20 and ~15 eV of the acceleration of beam 2 and of the deceleration of beam 1 (see Fig. 3) agree with the estimate.

The concentration of the electrons in the low-frequency wave is determined by the Boltzmann equation

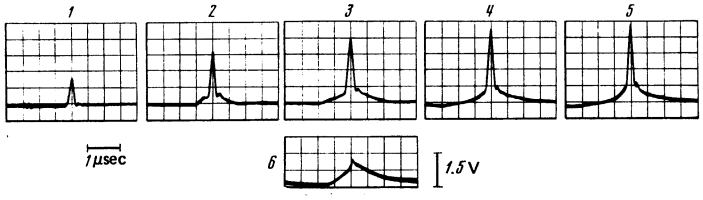

FIG. 6. Spatial evolution of solitary ion-density wave. Oscillograms 1–5 correspond to flight distances $x = 3$, 10, 20, 30, and 36 cm; curves 6—distribution of the potential in the wave.

$$n_e = n_0 \exp(e\varphi_m/T_e).$$

From the relation $e\varphi_m/T_e \approx 0$ 85 indicated above it follows that $n_e/n_0 \approx 2.4$, in qualitative agreement with the measurement results. From the ion-sound nature of the investigated shock wave it follows that the width of the front cannot be less than d_e. From this we can estimate the maximum ion density in the wave:

$$\varphi_m \approx T_e/e \approx 2\pi e(n_i - n_e)d_e^2,$$

i.e., $n_i \approx 3n_e$. If $n_e \approx 2.4n_0$, then the maximum ion density is $n_i \sim 7n_0$, i.e., it can exceed by serveral times the density of the unperturbed beam. Starting from the maximum values of the ion concentration in the solitary wave, we can estimate its formation time τ, i.e., the time of growth of the wave potential to the maximum value of φ_m. In a planar layer of width $\sim 2d_e$, an ion concentration n_i is accumulated on account of the arrival of particles from the two beams 1 and 2, moving with velocities $\Delta V/2$, i.e.,

$$2d_e n_i \approx 2n_0 \frac{\Delta V}{2}\tau,$$

and in the laboratory frame the flight distance over which the wave is formed is

$$L = V_0\tau \approx 2d_e \frac{V_0}{\Delta V}\frac{n_i}{n_0}.$$

At $V_0 = 2.5 \cdot 10^6$ cm/sec, $d_e = 0.1$ cm, $\Delta V = 5 \cdot 10^5$ cm/sec, $n_i/n_0 = 6$ this distance is $L \approx 6$ cm, in qualitative agreement with the experimentally observed value (Fig. 6).

Thus, the formation of the solitary wave at the point of the ion-beam velocity break is acccompanied by the appearance, during the amplitude growth, of a group of fast ions ($V > V_2$), which out-strip the wave, and slow ones ($V < V_1$), which lag the wave. In the stationary state, the two-velocity distribution of the particles ahead of the wave and behind its trailing edge can apparently be maintained on account of partial reflection of the ions by the wave fronts, i.e., continuous exchange of particles from the fast and slow beams in the field of the wave. The investigated solitary wave is analogous in fact to an ion-sound soliton with maximum amplitude φ_m in which the dissipation due to reflection of the particles of beam 1 by the leading front is offset by the symmetrical reflection of ions of beam 2 from the trailing edge.

3. When the velocity discontinuity ΔV exceeds $\sim 2.6C_s$ (see Fig. 4), a rather rapid transition is observed from a stationary solitary wave to a two-velocity distribution of the ions, i.e., interpenetration of beams 1 and 2. At the start of the flight path, near the ion source, there is also formed a nonstationary solitary wave with $M = 1.3$, and an accelerated group ("precursor") and a decelerated group of ions are produced. However, with increasing distance from the source, the amplitudes of the density and of the potential in the wave decrease, and the two beams become separated in velocity space. With increasing ΔV, the spatial region of the existence of the solitary wave shrinks and approaches the source. At large velocity-molulation amplitudes $\Delta V > 3C_s$ the spatial interpenetration of the beams (the region of the two-velocity regime) and the presence of groups of fast and slow ions are shown in Figs. 2 and 3.

CONCLUSION

The theory of collisionless electrostatic shock waves in an unmagnetized plasma was developed in Refs. 1 and 2. Laminar shock waves excited in the plasma by pulsed injection of an ion beam, and also by a jumplike increase of its velocity, were observed in experiment.[3-6] A computer experiment using the same formulation of the problem[4] has demonstrated the structure of the shock wave in the phase plane. In our study, where the shock wave was excited in a neutralized ion beam moving in vacuum, principal attention was paid to the dynamics of the establishment of the stationary state of the solitary wave, and to the possibility of obtaining a short dense ion cluster in such a system. The solitary wave, as indicated, is produced near the point where the beam has a velocity break at the optimal modulation amplitude $\Delta V \approx (2-3)C_s$. The fronts of the two ion-sound-like shock waves that move away along the beam from the break point, merge and form a solitary wave of larger amplitude, without changing its parameter while parameter while propagating with the beam. This effect can manifest itself, or can be used in various ion-beam systems, particularly beams of heavy ions (since the condition of realization of the considered processes is $V_0 < v_{Te}$). For example, random pulsations of relatively small amplitude of the voltage that accelerates the ions can lead to a deep modulation of the ion-beam current. The amplitude of these pulsations $\Delta U/U_0 \approx 2\Delta V/V_0$ is small at $\Delta V \approx 2.5C_s$:

$$\Delta U/U_0 \approx 3.5(T_e/eU_0)^{1/4},$$

Since in practice the value of T_e in the beams does not exceed several electron volts. On the other hand, using periodic small-amplitude pulsed modulation of the velocity it is possible to transform a continuous beam of ions into a sequence of short blobs that are comparable with the Debye length.

[1] S. S. Moiseev and R. Z. Sagdeev, Plasma Phys. (J. Nucl. Energy, Part C) **5**, 43 (1968).
[2] R. Z. Sagdeev, In: Voprosy teorii plazmy (Problems of Plasma Theory) No. 4, Atomizdat, 1964, p. 20.
[3] S. G. Alikhanov, V. G. Belan, and R. Z. Sagdeev, Pis'ma Zh. Eksp. Teor. Fiz. **7**, 405 (1968) [JETP Lett. **7**, 318 (1968)].
[4] H. Ikezi, T. Kamimura, M. Kako, and K. E. Lonngren, Phys. Fluids **16**, 2167 (1973).
[5] R. Z. Taylor, D. R. Baker, and H. Ikezi, Phys. Rev. Lett. **24**, 206 (1970).
[6] T. Honzawa, Plasma Phys. **15**, 467 (1973); **20**, 395 (1978).

Translated by J. G. Adashko